frontiers | Frontiers in Astronomy and Space Sciences

TYPE Original Research
PUBLISHED 24 October 2024
DOI 10.3389/fspas.2024.1458746

OPEN ACCESS

EDITED BY
Ritesh Patel,
Southwest Research Institute Boulder,
United States

REVIEWED BY
Vaibhav Pant,
Aryabhatta Research Institute of
Observational Sciences, India
Joan Burkepile,
National Center for Atmospheric Research
(UCAR), United States
Satabdwa Majumdar,
Austrian Space Weather Office, Austria

*CORRESPONDENCE
Yoichiro Hanaoka,
yoichiro.hanaoka@nao.ac.jp

RECEIVED 03 July 2024
ACCEPTED 10 October 2024
PUBLISHED 24 October 2024

CITATION
Hanaoka Y, Sakai Y and Masuda Y (2024)
High-accuracy polarization measurements of
the white-light corona during the 2023 total
solar eclipse.
Front. Astron. Space Sci. 11:1458746.
doi: 10.3389/fspas.2024.1458746

High-accuracy polarization measurements of the white-light corona during the 2023 total solar eclipse

Yoichiro Hanaoka[1,2]*, Yoshiaki Sakai[2,3] and Yukio Masuda[2]

[1]Solar Science Observatory, National Astronomical Observatory of Japan, Mitaka, Japan, [2]Solar Eclipse Digital Imaging and Processing Network, Tsukuba, Japan, [3]Chiba Prefectural Ichihara High School, Ichihara, Japan

This study measured the polarization of the white-light corona during the total solar eclipse on 20 April 2023, which occurred under high solar activity. The same instrument that was used for the 2017 and 2019 eclipse observations was employed, and despite the short duration of totality, the obtained data could be used for high-accuracy polarization analysis. We derived the brightness and polarization of the K + F corona and estimated the brightness distributions of the K- and F-coronae using polarization information. The polarization data of the corona are the key to estimating the amount of coronal hot plasma and its electron density distribution. Therefore, we examined the consistency between the eclipse data and those taken by the C2 coronagraph of the Large Angle Spectrometric Coronagraph (LASCO) on board the Solar and Heliospheric Observatory. Consequently, a systematic difference was observed; the polarization measured by LASCO-C2 was approximately 30% smaller than the results from the eclipse. Data from eclipses, which are captured under low background sky brightness and no scattered light due to the Sun's disk, can be a good calibration source of the brightness and polarization of the white-light corona.

KEYWORDS

sun, solar corona, while-light observation, polarimetry, total solar eclipses

1 Introduction

During a total solar eclipse, the solar white-light corona can be observed from immediately above the limb to several solar radii under a low sky-background level. X-ray and EUV observations of the corona, which are conducted by spacecraft every day, show coronal plasma at specific temperatures. In contrast, white-light observations map the density structure of the corona irrespective of the temperature. White-light corona is also regularly observed by coronagraphs. However, the spaceborne coronagraphs, such as the Large Angle Spectrometric Coronagraph (LASCO) (Brueckner et al., 1995) of the Solar and Heliospheric Observatory (SOHO), cannot observe the inner corona (typically <2 $R_{\odot}$) owing to the large occulting disk to block the light from the solar disk, and the ground-based ones, such as the Coronal Solar Magnetism Observatory K-coronagraph (K-Cor) (Hou et al., 2013) of the Mauna Loa Solar Observatory (MLSO), observes only the inner corona under a high sky-background level. Therefore, solar eclipses are still important for obtaining data of the white-light corona over a wide height range, though they occur only approximately twice every 3 years.

The white-light corona primarily comprises the K- and F-coronae, which represent the hot plasma produced by the Sun and interplanetary dust, respectively. The electron density distribution of coronal hot plasma, which is an important piece of fundamental information about the corona, can be derived from the brightness distribution of the K-corona, as proposed by van de Hulst (1950). Therefore, to study the distribution of coronal hot plasma, the K- and F-coronae should be quantitatively separated. This can be done using polarization imaging data of the white-light corona because the K-corona, wherein radiation is produced by Thomson scattering, exhibits polarization, whereas the F-corona does not exhibit polarization up to several solar radii (see Lamy et al., 2021, references therein). Therefore, coronagraphs for white-light observation, both ground-based and spaceborne, can measure polarization.

Polarimetry has also been performed during total solar eclipses. Recently digital instruments have been used for polarimetry. Capobianco et al. (2012) observed the 2006 eclipse using an 'E-Kpol' polarimeter and Skomorovsky et al. (2012) observed the 2008 eclipse using a triple-polarized-image telescope. In particular, during the total eclipse of 2017, wherein the path of totality passed the mainland of the United States of America, many observers challenged polarization measurements, and certain successful results were reported (Judge et al., 2019; Vorobiev et al., 2020; Bemporad, 2020; Liang et al., 2023). Similar observations were made during the subsequent eclipses (Liberatore et al., 2023 for the 2019 eclipse; Edwards et al., 2023 for the 2020 eclipse). We also succeeded in conducting polarimetry at multiple sites during the 2017 and 2019 eclipses (Hanaoka et al., 2021).

The derivation of the electron density distribution of the corona has been attempted in certain of the above eclipse studies as well as using spaceborne coronagraphs (e.g., Hayes et al., 2001; Quémerais and Lamy, 2002). To derive the correct electron densities, well-calibrated brightness data for the K-corona are required. Fortunately, the accuracy of polarimetry has significantly improved in recent digital observations. For example, the above-mentioned results for the 2017 eclipse show good agreement; in particular, the consistency between the results by Vorobiev et al. (2020) and those by Hanaoka et al. (2021) is remarkable (Figure 7 in Hanaoka et al., 2021).

However, a systematic discrepancy between the polarimetry results was observed for the data obtained during the 2017 and 2019 eclipses and those captured with LASCO-C2 (one of the coronagraphs comprising LASCO covering up to 6.5 $R_\odot$) on the eclipse days (Hanaoka et al., 2021). The polarizations measured by LASCO-C2 were systematically lower than those measured during the eclipses by approximately 30%. A comparison between the eclipse results and those obtained by LASCO-C2 was possible because our observations had a wide field-of-view covering up to approximately 4 $R_\odot$, unlike most of the other eclipse observations, which covered only the inner corona $< 2\ R_\odot$. The consistency among the polarimetry results for the corona should be investigated further to study the distribution of the coronal plasma, and wide-field eclipse data will contribute to this.

We observed a total solar eclipse in Australia in 2023 to obtain polarimetry data. We used the same instrument that was used for the 2017 and 2019 eclipses. Although the duration of totality of the 2023 eclipse was less than 1 min, we successfully obtained data from which we could derive high-accuracy polarization signals. This paper presents the results of the polarimetry performed during the 2023 eclipse.

This study is a repetition of the analyses performed for the 2017 and 2019 eclipses. However, not only is it a wide field-of-view record of the corona during the 2023 eclipse, but it also has other significant advantages.

1. Eclipse polarimetry data are often calibrated using the polarization brightness measured by K-Cor of MLSO. However, during the 2023 eclipse, K-Cor was not working, and in such cases, reference data other than the K-Cor data are required. The COR1 coronagraph of Solar Terrestrial Relations Observatory/Sun Earth Connection Coronal and Heliospheric Investigation (Howard et al., 2008), which was located near the Earth during the 2023 eclipse, measured the brightness and polarization of the corona during the eclipse. However, the COR1 data show considerable errors particularly in the inter-streamer low light-level regions, as indicated by Frazin et al. (2012). Therefore, the accuracy of the calibration using the COR1 data is presumed to be limited. We can calibrate the data using our solar disk images captured along with eclipse images.
2. In contrast to the 2017 and 2019 eclipses, which occurred in the declining phase and near the minimum solar activity, the 2023 eclipse occurred during high solar activity. As previously stated, a discrepancy between the polarimetry results was observed in the 2017 and 2019 eclipses. We can check whether the same tendency is observed in the results obtained under high solar activity.

The remainder of this paper is organized as follows. The observations of the 2023 eclipse and reduction for the obtained data are described in Section 2. The measurement results of the brightness and polarization of the K + F corona and the respective brightness distributions of the K- and F-coronae estimated from the polarimetry data are presented in Section 3. Section 4 is devoted to a summary and discussion including a comparison between the eclipse data and LASCO-C2 measurements for the 2023 eclipse as well as the 2017 and 2019 eclipses.

2 Observations and data reduction

The observation and reduction methods were similar to those employed in the study of the 2017 and 2019 eclipses described by Hanaoka et al. (2021). Therefore, we briefly present them here.

2.1 Observations

The observations were conducted under professional-amateur collaborations for eclipse observations, which produced scientific results for former eclipses (Hanaoka et al., 2012; 2014; 2018; 2021). We conducted the observations of the 2023 eclipse on 20 April 2023, at Exmouth of Western Australia, Australia (21.93S, 114.13E) in clear weather. The maximum eclipse occurred at 03:30:17 UT at an altitude of 54.3° and the duration of totality was 56 s.

The polarimetry instrument comprised a 60-mm refractor (Takahashi FS-60Q; focal length = 600 mm), a filter turret (fabricated by Koheisha, Kawagoe, Japan), and a digital single-lens reflex camera (DSLR; Canon EOS6D). The filter turret was equipped with three linear polarizers with transmission axis orientations of 0°, 60°, and 120°, and a neutral density filter to obtain ordinary images. The turret underwent two complete rotations during totality, and coronal images were taken twice at each of the four filter positions. At each position, five images with exposure times of 1/2, 1/8, 1/32, 1/128, and 1/512 s were taken to cover the wide brightness range of the white-light corona. In addition to polarization imaging, ordinary imaging observations were performed using other small telescopes and commercial cameras.

The instruments had a wide field-of-view covering 4 $R_\odot$ or greater from the solar disk-center and were mostly free from ghosting (artifact images of the very bright inner corona produced by internal reflections of the lenses). Ghosting hinders the measurement of the coronal brightness in areas distant from the Sun. In particular, the polarimetry accuracy is severely affected by ghosting. Using our instruments, we can perform reliable photometry and polarimetry down to low brightness levels.

In addition to the coronal images acquired during totality, images of the solar disk before the first contact and after the fourth contact of the eclipse and images of the partially eclipsed Sun were also taken using additional neutral density filters. Solar disk images were used to calibrate the brightness of the corona with respect to the mean brightness of the disk. As stated above, such calibration data are required for the 2023 eclipse, when the K-Cor data are not available. We performed the calibrations using the solar disk images for the data taken during the former eclipses, even when the K-Cor data were available, because the calibration could be performed free from the possible error of the K-Cor data caused by the bright background sky.

2.2 Data reduction

Images captured with each of the polarizers and the ND filter were stacked to produce a single, wide dynamic-range, low-noise map. Each map was produced from a set of ten images (five different exposure times × two rotations). First, dark and flat corrections were applied. We took images of the sky with the polarizers and the ND filter to obtain their respective flat-field data. To eliminate the influence of the polarization and brightness gradient of the sky, we took flat-field data rotating the telescope around its optical axis. In addition, we took images using a light diffuser with pointing the telescope to the Sun (an unpolarized light source) to examine the throughput differences among the polarizers; we corrected up to 0.6% differences in the throughputs.

Furthermore, before the image stacking, certain preparations were required as described below.

1. Derivation of the positional shifts of the Sun in images. The position of the Sun's disk center on the raw images fluctuated due to tracking errors and wind effects. Because the solar disk is hidden by the Moon, the shifts in the images were derived by referencing fine coronal structures.
2. Conversion from the data number of raw images to those showing the amount of incident light (brightness of the corona) per second. Basically, the amount of incident light and analog-to-digital converted data number (dark level removed) show a linear relationship. However, certain cameras, including the one used for our polarimetry observation, show a non-linear response. This non-linearity can be examined comparing two images of the solar corona captured at different exposure times. We derived a non-linear function and corrected the raw data numbers of the images. In addition, we estimated the true ratio of the exposure times. The exposure times were 1/2, 1/8, ..., 1/512 s, and the ratio of the adjacent exposure times was nominally 4. However, systematic errors may occur because the shutter is a mechanical device. A comparison of two images with different exposure times (non-linearity corrected) also provides the true ratio of the exposure times. With the corrected exposure times, the data numbers were converted into numbers per second.
3. Images captured at various exposure times have respective brightness ranges that were properly exposed because the dynamic range of the coronal brightness extends over several orders of magnitude. Before stacking the images, underexposed and overexposed parts were discarded.

At this stage, the corrections of the non-linearity and exposure-time errors were applied to the flat-field data, and all the raw images were corrected with the new flat-field. With these newly corrected images, the non-linearity and exposure-time errors were again examined. Following the above preparations, we stacked the images and obtained wide dynamic-range maps for the three polarizers and ND filter.

Certain stars can be found in the stacked maps, and their positions can be found in the Hipparcos catalog (http://archive.eso.org/skycat/servers/ASTROM). Using these stars as a reference, we derived the position of the center of the solar disk, the direction of the solar north, and the pixel scale ($2''.26$ pixel^{-1}) in the maps.

To measure the brightness of the solar disk, which is the reference for coronal brightness, we calculated the data number of the disk image without the additional ND filters used to capture the disk images. The effective transmissions of the ND filters were calculated by combining the spectral transmissions of the ND filters, solar spectrum, and spectral response curve of the camera. We checked the variation in the transparency of the atmosphere from the start to the end of the eclipse using the full-disk images and the partial eclipse images, and estimated the disk brightness during totality, which was used as the reference for brightness.

By combining the stacked maps for the three polarizer positions, we obtained the Stokes *I*, *Q*, and *U* signals of the corona, and converted their units to the mean brightness of the solar disk. These Stokes parameters can be easily converted into expressions of the polarization often used for the corona, namely, the polarization brightness, orientation of the linear polarization, and degree of polarization.

The camera used for polarimetry was a commercial DSLR camera, which can capture images of three (red, green, and blue, or R, G, and B) color channels, with central wavelengths of approximately 600, 530, and 470 nm, respectively. Image stacking and brightness calibration were independently performed for each channel, and we obtained brightness and polarization distribution data for the R, G, and B channels.

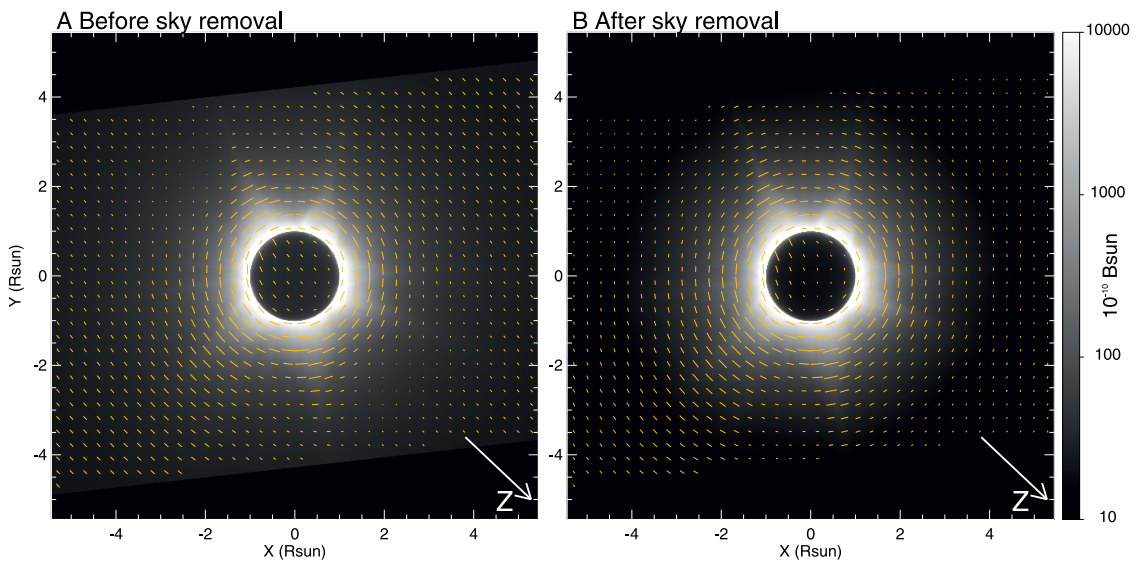

FIGURE 1
White-light polarization maps of the G-channel covering 9.2 × 9.2 $R_\odot$ area **(A)** before and **(B)** after the removal of the sky background taken during the 2023 total solar eclipse. The degree and orientation of the linear polarization signals are presented with orange ticks, and the grayscale images show Stokes *I* signals. The solar north is to the top, and the arrows represent the direction of the zenith.

Ordinary white-light imaging data of the corona obtained with the other telescopes and cameras (not equipped with polarizers) were processed in a similar manner and used to check the consistency of the brightness calibration.

3 Results

The distributions of the derived polarization signals are shown in Figure 1. Figure 1A shows the raw polarization signals (orange ticks) plotted on a coronal image (gray scale). The raw polarization signals include the sky background, which shows the polarization approximately along the zenith-horizon direction (the zenith direction is indicated with arrows in the Figure). The polarization signals distant from the Sun in Figure 1A are dominated by the sky component.

The brightness and polarization of the sky were estimated as follows. The linear polarization signals of the corona are tangential to the Sun. Therefore, after the removal of the appropriate polarization of the sky (assumed to be constant in the field of view), only the tangential polarization signals remain. In the outermost area in the field of view, the K-corona is very weak, and therefore, the observed brightness comprises the components of the sky and the F-corona. On the assumption that the degree of polarization of the sky does not depend on the wavelength and the spectral distribution of the F-corona is $\lambda^{0.91}$ (Boe et al., 2021), we estimated the brightness of the sky using the data of the RGB channels.

Figure 1B shows a map of the K + F corona after removing thus derived sky background. Tangentially aligned linear polarization signals produced by the K-corona were observed. The brightness of the corona presented in Figures 1A,B is expressed in units of the mean brightness of the solar disk ($B_\odot$). We checked the consistency of the brightness calibration between the polarimetry data and other independently calibrated imaging data. The brightness differences were within 7% for the inner corona in channels R, G, and B.

Figure 2 presents an enlarged view of polarization parameters of part of the inner K + F corona, demonstrating the quality of the polarization measurements. Figure 2A shows the brightness distribution of the K + F corona and Figure 2B shows the distribution of the degree of polarization. Figure 2A shows some high-lying prominences denoted by arrows. Unlike the low-lying saturated prominences, the polarization signals of the high-lying prominences were measured correctly. Figure 2B shows that the degree of polarization of these prominences (also denoted by arrows) was lower than that of the surrounding corona. This is because the prominences emit unpolarized free-bound and free-free radiation in addition to Thomson-scattering light (Jejčič et al., 2018). Figure 2B does not show spurious signals around the prominences caused by insufficient alignment corrections.

Figure 2C shows the deviation in the orientation of the linear polarization signals from the tangential direction. Pixel-wise random errors were found in the corona; however, no systematic errors, which are caused by errors in polarization calibration and/or brightness and polarization estimation of the sky, were observed. In fact, the average unsigned error of the orientation angle of the linear polarization signals within 1.2 $R_\odot$ was as small as approximately 0.15°. This approximately corresponds to a 0.5% error in the Stokes *Q* and *U* signals. At 2 $R_\odot$ and 3 $R_\odot$, the systematic error increases to 0.4° and 1.1°, which corresponds to 1.5% and 3.5% errors in the *Q* and *U* signals. As shown in Figure 2, a high accuracy was achieved in our polarization measurements.

Figure 3 shows the brightness (B_{K+F}, upper curves in each panel) and polarization brightness (pB, lower curves) of the K + F corona for the R, G, and B channels at several elongations. The position angle was measured counterclockwise from the solar

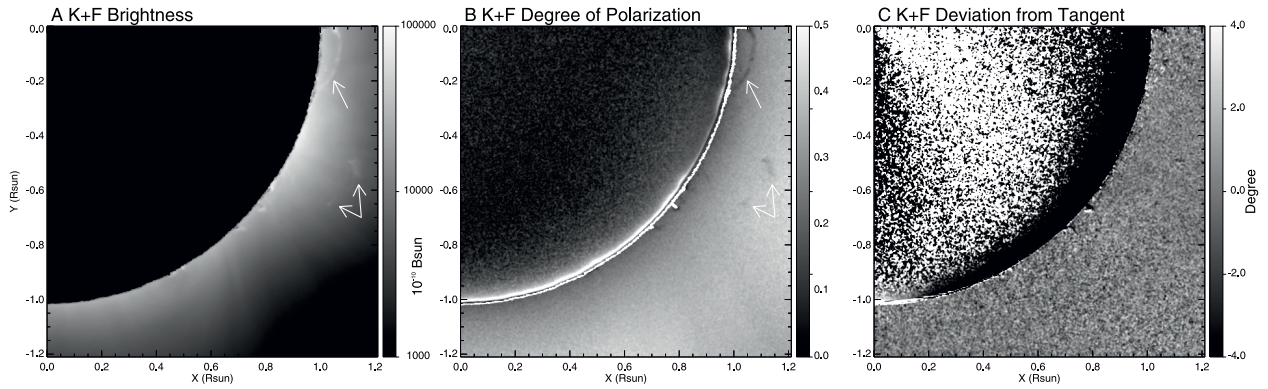

FIGURE 2
Maps showing polarization parameters in the southwest quadrant of the inner K + F corona. Panels **(A)**, **(B)**, and **(C)** show the brightness distribution, distribution of the degree of polarization, and deviation in the orientation of the linear polarization signals from the tangential direction, respectively. There are certain high-lying prominences denoted by arrows in **(A)** and **(B)**.

north. The plotted values were averaged over an area of 15″.8 × 15″.8. These plots are drawn in a manner similar to that in Figures 5 and 6 of Hanaoka et al. (2021), which show the results for the 2017 and 2019 eclipses, respectively. The measured brightness and polarization during the 2017 and 2019 eclipses are also presented with filled area plots. Compared to these former eclipses, where the bright regions concentrate around the equator, we found that the B_{K+F} and pB in 2023 were dominated by enhancements due to coronal streamers because of the high solar activity.

As previously stated, the polarization signals originate only from the K-corona. The polarization parameters shown in Figures 1B, 2, 3 are the sum of the K- and F-coronae; however, we can discriminate them using the polarization brightness pB. The brightness of the K- and F-coronae, B_K and B_F, can be expressed as $B_F = B_{K+F} - B_K$ and $B_K = pB/p_K$, where p_K is the degree of polarization of the K-corona alone. Therefore, based on the assumption of a plausible p_K, we can derive B_K and then B_F. As described by Hanaoka et al. (2021), a plausible p_K at each elongation can be estimated as follows. Assuming the spherically symmetric distribution of electron density in the corona, p_K is constant at each elongation. In the inner corona (<2 $R_\odot$), the F-corona is approximately circularly distributed (e.g., Saito et al., 1977; see also Koutchmy and Lamy, 1985). Therefore, it is presumed that the correct p_K at a certain elongation yields a constant B_F ($= B_{K+F} - pB/p_K$) regardless of the position angle. Beyond 2 $R_\odot$, the F-corona becomes elliptical; therefore, p_K estimation assuming a circular F-corona is impossible. However, beyond 2 $R_\odot$, p_K becomes approximately constant regardless of the elongation, because the solar disk, which is the light source for Thomson scattering, can be considered a point source beyond 2 $R_\odot$. We assumed that p_K above 2 $R_\odot$ was the same as that derived at 2 $R_\odot$.

Figure 4 shows the approximate distributions of the K- and F-coronae derived based on thus estimated p_K. Whereas the K-corona mostly comprised many streamers, the F-corona basically exhibited a structureless brightness distribution. However, there was certain unevenness in the F-corona around the streamer positions seen in the K-corona. Streamers are local high-electron-density structures that break the spherical symmetry of electron density. Therefore, to be accurate, p_K was not constant for any elongation. An error in p_K produces apparent unevenness in the F-corona. An attempt has been made to derive more realistic brightness distributions of the K- and F-coronae based on the three-dimensional streamer structures (Burtovoi et al., 2022). If the three-dimensional directions of streamers during eclipses can be determined from coronagraph observations, more reliable discrimination of the K- and F-coronae becomes possible. However, the distributions of the K- and F-coronae derived based on simple assumptions are considered reasonable.

4 Summary and discussion

We successfully obtained well-calibrated total brightness B_{K+F} and polarization brightness pB of the corona from immediately above the limb to approximately 4 $R_\odot$ during the 2023 solar eclipse, despite the short duration of totality. The high accuracy of the polarization measurements was demonstrated. Furthermore, we presented the approximate distributions of B_K and B_F.

Our eclipse data covering a wide field-of-view can be compared with the data of the outer white-light corona, such as those obtained by LASCO-C2 of SOHO, which covers the corona in the range of 2.5–6.5 $R_\odot$. Hanaoka et al. (2021) found that the brightness of the K + F corona derived from the 2017 and 2019 eclipse data and that measured by LASCO-C2 agreed well, indicating that the brightness calibrations were performed appropriately. However, as mentioned previously, they also found a systematic difference between the polarization data obtained during eclipses and those obtained by LASCO-C2.

The 2017 and 2019 eclipses occurred under low solar activity. We then compared the results of the 2023 eclipse, which occurred under high solar activity, with those of LASCO-C2. LASCO-C2 data were obtained from the "LASCO-C2 Legacy Archive" (http://idoc-lasco.ias.u-psud.fr/sitools/client-portal/doc/; refer to Lamy et al., 2020). Figure 5 shows the radial distribution of the brightness (B_{K+F}, panels A–C) and degree of polarization (p_{K+F}, panels D–F) of the K + F corona derived from the 2017, 2019, and 2023 eclipse data (black lines) and those measured by LASCO-C2 on the same

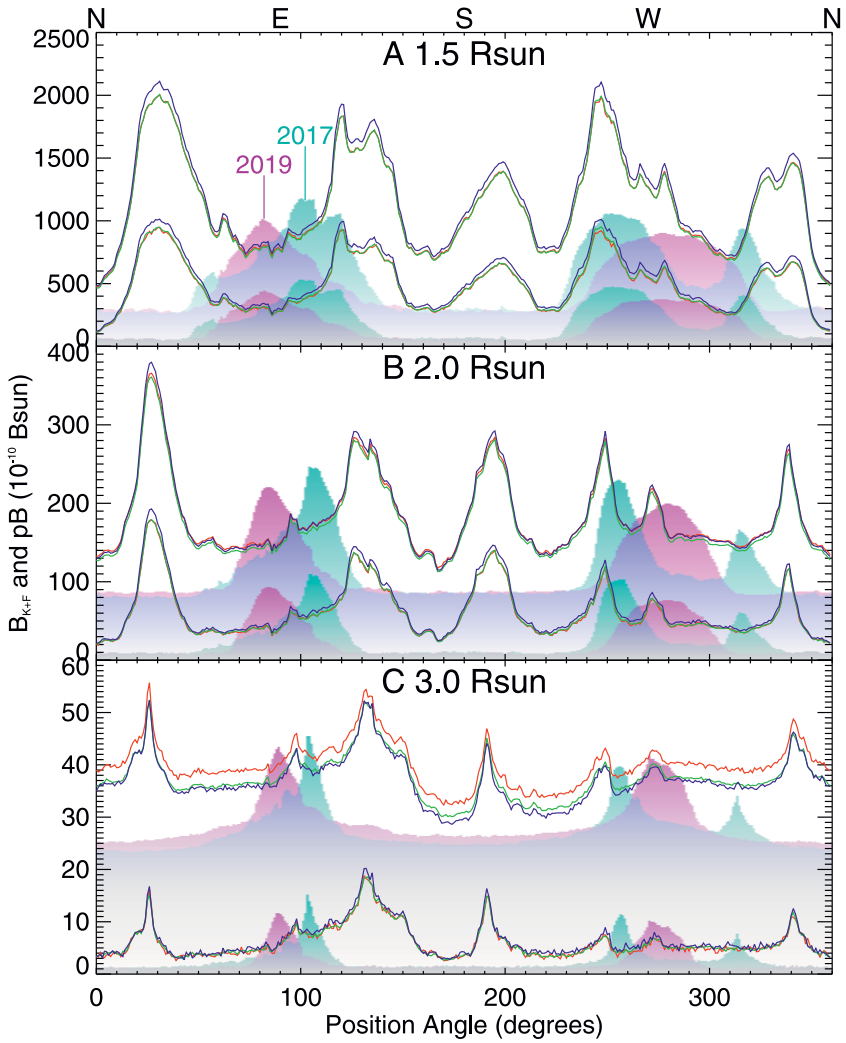

FIGURE 3
Position angle distributions of the total brightness of the K + F corona (B_{K+F}, upper curves) and its polarization brightness (pB, lower curves) at elongations of 1.5, 2.0, and 3.0 $R_\odot$ observed during the 2023 eclipse. The R, G, and B channels are represented by red, green, and blue lines, respectively. Filled area plots in the background present the brightness and polarization measured during the 2017 (cyan) and 2019 (magenta) eclipses.

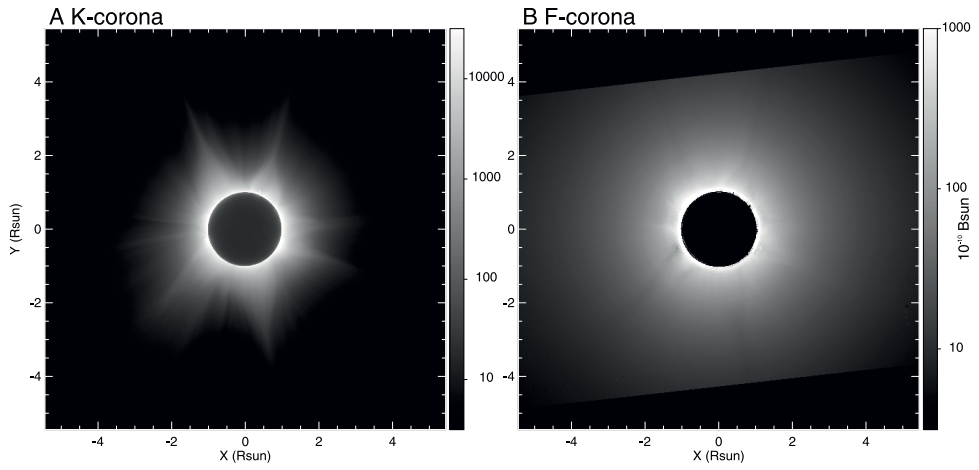

FIGURE 4
Gray-scale maps of **(A)** the K-corona and **(B)** the F-corona for the area shown in Figure 1.

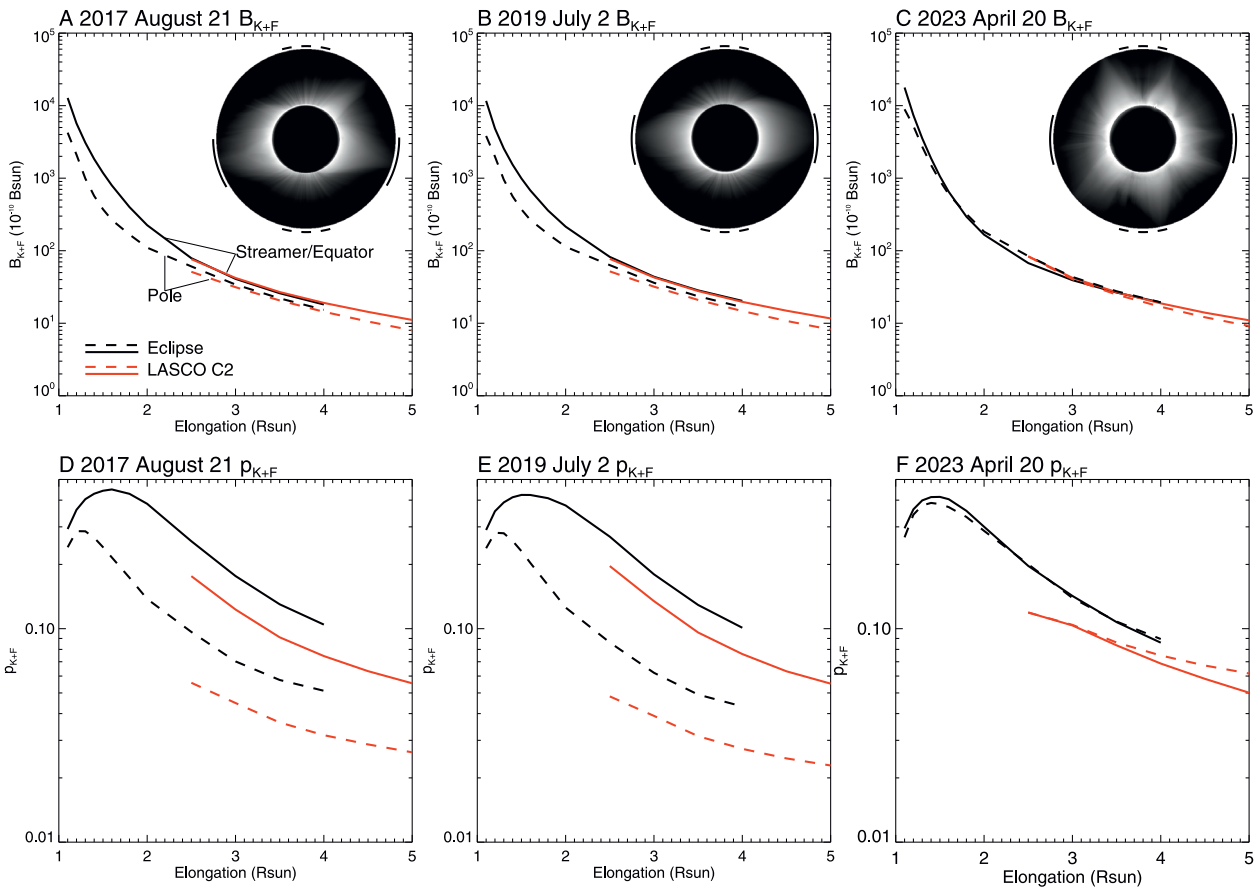

FIGURE 5
Panels **(A–C)** present the comparison of the radial distribution of the brightness of the K + F corona (B_{K+F}) of the equator or equatorial streamers (solid lines) and the poles (dashed lines) between our eclipse observations (black) and the LASCO-C2 observations (red) for the 2017, 2019, and 2023 eclipses. The inset images show the white-light corona captured during the respective eclipses, and the arcs indicate the ranges treated as equator/streamers (solid arcs) or those treated as poles (dashed arcs). Panels **(D–F)** show the comparison of the degree of polarization (p_{K+F}) in the same manner. The eclipse data are the averages of the R and G channels.

days as the eclipses (red lines). The eclipse data were averages of the R and G channels, which covered the filter bandpass of LASCO-C2 of 540–640 nm. The averages within ±15° of the position angle around the equator or equatorial streamers (solid lines) and the north and south poles (dashed lines) are presented in Figure 5. The position-angle ranges treated as equator/streamers (solid arcs) or poles (dashed arcs) are shown in the insets of Figure 5. As shown in Figure 4, the corona during the 2023 eclipse showed the streamers extending in various directions, as typically observed in the corona near the solar maximum. Therefore, the equator and poles do not correspond to either major streamers or quiet, streamerless corona; Figures 5C, F show no clear differences between the equator and poles. For all three eclipses, we found a gap in the degree of polarization between the eclipse data and LASCO-C2 measurements, whereas the B_{K+F} of the eclipse and LASCO-C2 agreed well, regardless of the solar activity level. The degree of polarization of LASCO-C2 was approximately 30% lower than that of the eclipse. As discussed by Hanaoka et al. (2021), the possible error in the estimation of the sky component cannot explain this 30% difference.

The results in Figure 5 indicate that there is a discrepancy in the polarization brightness, pB ($= B_{K+F} \times p_{K+F}$), which represents the coronal hot plasma. Incorrect pB values cause errors in the estimation of the amount of coronal hot plasma and its electron density distribution. If this discrepancy is resolved, the polarization data of the eclipses and those of LASCO-C2 can be combined. The combined results provide the B_K distribution from immediately above the limb to approximately 6 $R_\odot$, and we can derive the electron density distribution of the corona over wide range.

These results highlight the importance of eclipse observations in the present day. Total solar eclipses provide a well-calibrated brightness distribution of the corona over a wide height range under very small disturbances, and such data are difficult to acquire using other methods. The eclipse data can also be used as a good calibration source for the brightness and polarization of the white-light corona, not only for existing coronagraphs, but also for future missions.

To render the data useable for intercomparison among the observations to further check consistency, we have presented our

data of the 2023 eclipse along with those of the 2017 and 2019 eclipses at https://solarwww.mtk.nao.ac.jp/mitaka_solar/solar_eclipse/polarization/.

Data availability statement

The datasets presented in this study can be found in online repositories. The names of the repository/repositories and accession number(s) can be found below: http://archive.eso.org/skycat/servers/ASTROM (the Hipparcos catalog), http://idoc-lasco.ias.u-psud.fr/sitools/client-portal/doc/ (the LASCO-C2 Legacy Archive). The datasets generated for this study can be found in: https://solarwww.mtk.nao.ac.jp/mitaka_solar/solar_eclipse/polarization/ (Solar Science Observatory, National Astronomical Observatory of Japan).

Author contributions

YH: Conceptualization, Formal Analysis, Methodology, Writing–original draft, Writing–review and editing. YS: Investigation, Writing–review and editing. YM: Investigation, Writing–review and editing.

Funding

The author(s) declare that no financial support was received for the research, authorship, and/or publication of this article.

Acknowledgments

Mr. Shin-ichiro Mishima also joined the professional-amateur collaborative observations and succeeded to take coronal images and provided us the data. This work makes use of the LASCO-C2 legacy archive data produced by the LASCO-C2 team at the Laboratoire d'Astrophysique de Marseille and the Laboratoire Atmosphères, Milieux, Observations Spatiales, both funded by the Centre National d'Etudes Spatiales (CNES). LASCO was built by a consortium of the Naval Research Laboratory, United States, the Laboratoire d'Astrophysique de Marseille (formerly Laboratoire d'Astronomie Spatiale), France, the Max-Planck-Institut für Sonnensystemforschung (formerly Max Planck Institute für Aeronomie), Germany, and the School of Physics and Astronomy, University of Birmingham, United Kingdom SOHO is a project of international cooperation between ESA and NASA.

Conflict of interest

The authors declare that the research was conducted in the absence of any commercial or financial relationships that could be construed as a potential conflict of interest.

Publisher's note

References

Bemporad, A. (2020). Coronal electron densities derived with images acquired during the 2017 august 21 total solar eclipse. *Astrophys. J.* 904, 178. doi:10.3847/1538-4357/abc482

Boe, B., Habbal, S., Downs, C., and Druckmüller, M. (2021). The color and brightness of the F-corona inferred from the 2019 july 2 total solar eclipse. *Astrophys. J.* 912, 44. doi:10.3847/1538-4357/abea79

Brueckner, G. E., Howard, R. A., Koomen, M. J., Korendyke, C. M., Michels, D. J., Moses, J. D., et al. (1995). The large angle spectroscopic coronagraph (LASCO). *Sol. Phys.* 162, 357–402. doi:10.1007/BF00733434

Burtovoi, A., Naletto, G., Dolei, S., Spadaro, D., Romoli, M., Landini, F., et al. (2022). Measuring the F-corona intensity through time correlation of total and polarized visible light images. *Astron. Astrophys.* 659, A50. doi:10.1051/0004-6361/202141414

Capobianco, G., Fineschi, S., Massone, G., Balboni, E., Malvezzi, A. M., Crescenzio, G., et al. (2012). Electro-optical polarimeters for ground-based and space-based observations of the solar K-corona. *Mod. Technol. Space- Ground-based Telesc. Instrum. II* 8450, 845040. doi:10.1117/12.926896

Edwards, L., Bunting, K. A., Ramsey, B., Gunn, M., Fearn, T., Knight, T., et al. (2023). Derived electron densities from linear polarization observations of the visible-light corona during the 14 december 2020 total solar eclipse. *Sol. Phys.* 298, 140. doi:10.1007/s11207-023-02231-5

Frazin, R. A., Vásquez, A. M., Thompson, W. T., Hewett, R. J., Lamy, P., Llebaria, A., et al. (2012). Intercomparison of the LASCO-C2, SECCHI-COR1, SECCHI-COR2, and Mk4 coronagraphs. *Sol. Phys.* 280, 273–293. doi:10.1007/s11207-012-0028-3

Hanaoka, Y., Hasuo, R., Hirose, T., Ikeda, A. C., Ishibashi, T., Manago, N., et al. (2018). Solar coronal jets extending to high altitudes observed during the 2017 august 21 total eclipse. *Astrophys. J.* 860, 142. doi:10.3847/1538-4357/aac49b

Hanaoka, Y., Kikuta, Y., Nakazawa, J., Ohnishi, K., and Shiota, K. (2012). Accurate measurements of the brightness of the white-light corona at the total solar eclipses on 1 august 2008 and 22 july 2009. *Sol. Phys.* 279, 75–89. doi:10.1007/s11207-012-9984-x

Hanaoka, Y., Nakazawa, J., Ohgoe, O., Sakai, Y., and Shiota, K. (2014). Coronal mass ejections observed at the total solar eclipse on 13 november 2012. *Sol. Phys.* 289, 2587–2599. doi:10.1007/s11207-014-0476-z

Hanaoka, Y., Sakai, Y., and Takahashi, K. (2021). Polarization of the corona observed during the 2017 and 2019 total solar eclipses. *Sol. Phys.* 296, 158. doi:10.1007/s11207-021-01907-0

Hayes, A. P., Vourlidas, A., and Howard, R. A. (2001). Deriving the electron density of the solar corona from the inversion of total brightness measurements. *Astrophys. J.* 548, 1081–1086. doi:10.1086/319029

Hou, J., de Wijn, A. G., and Tomczyk, S. (2013). Design and measurement of the Stokes polarimeter for the COSMO K-coronagraph. *Astrophys. J.* 774, 85. doi:10.1088/0004-637X/774/1/85

Howard, R. A., Moses, J. D., Vourlidas, A., Newmark, J. S., Socker, D. G., Plunkett, S. P., et al. (2008). Sun Earth connection coronal and heliospheric investigation (SECCHI). *Space Sci. Rev.* 136, 67–115. doi:10.1007/s11214-008-9341-4

Jejčič, S., Kleint, L., and Heinzel, P. (2018). High-density off-limb flare loops observed by SDO. *Astrophys. J.* 867, 134. doi:10.3847/1538-4357/aae650

Judge, P., Berkey, B., Boll, A., Bryans, P., Burkepile, J., Cheimets, P., et al. (2019). Solar eclipse observations from the ground and air from 0.31 to 5.5 microns. *Sol. Phys.* 294, 166. doi:10.1007/s11207-019-1550-3

Koutchmy, S., and Lamy, P. L. (1985). "The F-corona and the circum-solar dust evidences and properties [G. Nikolsky memorial lecture]," in *The F-corona and the circum-solar dust evidences and properties (ir)*, 63, 63–74. doi:10.1007/978-94-009-5464-9_14

Lamy, P., Gilardy, H., Llebaria, A., Quémerais, E., and Ernandez, F. (2021). LASCO-C3 observations of the K- and F-coronae over 24 Years (1996 - 2019): photopolarimetry and electron density distribution. *Sol. Phys.* 296, 76. doi:10.1007/s11207-021-01819-z

Lamy, P., Llebaria, A., Boclet, B., Gilardy, H., Burtin, M., and Floyd, O. (2020). Coronal photopolarimetry with the LASCO-C2 coronagraph over 24 Years [1996 - 2019]. *Sol. Phys.* 295, 89. doi:10.1007/s11207-020-01650-y

Liang, Y., Qu, Z., Hao, L., Xu, Z., and Zhong, Y. (2023). Imaging-polarimetric properties of the white-light inner corona during the 2017 total solar eclipse. *Mon. Not. R. Astron. Soc.* 518, 1776–1788. doi:10.1093/mnras/stac3183

Liberatore, A., Zender, J., Capobianco, G., Fineschi, S., Panasenco, O., Tomuta, D., et al. (2023). Polarimetric study of the solar corona during the total solar eclipse on july 2, 2019 with a liquid-crystal polarimeter. *Sol. Phys.* 298, 85. doi:10.1007/s11207-023-02175-w

Quémerais, E., and Lamy, P. (2002). Two-dimensional electron density in the solar corona from inversion of white light images - application to SOHO/LASCO-C2 observations. *Astron. Astrophys.* 393, 295–304. doi:10.1051/0004-6361:20021019

Saito, K., Poland, A. I., and Munro, R. H. (1977). A study of the background corona near solar minimum. *Sol. Phys.* 55, 121–134. doi:10.1007/BF00150879

Skomorovsky, V. I., Trifonov, V. D., Mashnich, G. P., Zagaynova, Y. S., Fainshtein, V. G., Kushtal, G. I., et al. (2012). White-light observations and polarimetric analysis of the solar corona during the eclipse of 1 august 2008. *Sol. Phys.* 277, 267–281. doi:10.1007/s11207-011-9910-7

van de Hulst, H. C. (1950). The electron density of the solar corona. *Bull. Astron. Inst. Neth.* 11, 135.

Vorobiev, D., Ninkov, Z., Bernard, L., and Brock, N. (2020). Imaging polarimetry of the 2017 solar eclipse with the RIT polarization imaging camera. *Publ. Astron. Soc. Pac.* 132, 024202. doi:10.1088/1538-3873/ab55f1